Approaching the conformal WZW behavior in the infrared limit of two-dimensional massless QCD: A lattice study

Nikhil Karthik*
American Physical Society, Hauppauge, New York 11788, USA
and Department of Physics, Florida International University, Miami, Florida 33199, USA

Rajamani Narayanan†
Department of Physics, Florida International University, Miami, Florida 33199, USA

Sruthi A. Narayanan‡
Perimeter Institute for Theoretical Physics, Waterloo, Ontario N2L 2Y5, Canada

(Received 3 January 2024; accepted 21 February 2024; published 12 March 2024)

Two-dimensional QCD with N_c colors and N_f flavors of massless fermions in the fundamental representation is expected to exhibit conformal behavior in the infrared governed by a $u(N_f)$ Wess–Zumino–Witten model with level N_c. Using numerical analysis within the lattice formalism with exactly massless overlap fermions, we show the emergence of such behavior in the infrared limit. Both the continuum extrapolated low-lying eigenvalues of the massless Dirac operator and the propagator of scalar mesons exhibit a flow from the ultraviolet to the infrared. We find that the amplitude of the conserved current correlator remains invariant under the flow, while the amplitude of the scalar correlator approaches N_f-independent values in the infrared.

DOI: 10.1103/PhysRevD.109.054502

I. INTRODUCTION

Two-dimensional QCD serves as an interesting toy model to study emergent conformal behavior in the infrared. As long as the number of colors, $N_c > 1$, is finite, the $su(N_c)$ gauge theory with N_f flavors of massless fermions in the fundamental representation has a conformal sector in the infrared limit [1]. The identification of which two-dimensional conformal field theory (CFT) describes the massless sector of the theory is somewhat of a conjecture. An ab initio numerical study of the infrared limit of QCD and verification of the existing expectation that the long-distance behavior of two-dimensional QCD is described by an appropriate Wess–Zumino–Witten (WZW) model is the aim of this paper.

Two-dimensional QCD is usually studied in the Hamiltonian formalism, and light-cone gauge serves as a convenient choice to work in. With this gauge choice, in addition to the gauge field being constrained, the fermion of one chirality (e.g., the right-chiral ψ_R) is also constrained, leaving the dynamics to be governed by a left-chiral fermion ψ_L. It is additionally advantageous to work on the light-cone as the momentum takes on only positive values, which become discrete if the direction perpendicular to the propagation direction is compact. This enables one to study the problem numerically via the method referred to as the Discrete Light-Cone Quantization (DLCQ) [2,3]. The flavor current constructed from the left-chiral fermion commutes with the interacting Hamiltonian, which fully describes the dynamics in the massless limit. Therefore, the states formed by repeatedly acting on the vacuum with flavor current operators are massless states. However, the flavor currents formed by the constrained right-chiral fermions do not commute with the Hamiltonian, and we do not have a proper description of the conformal behavior such as that given by a WZW model.

Instead, if one considers the theory not on the light front in order to take all degrees of freedom into account, one could conjecture [1] that the infrared description is from a WZW model. The basis of this statement comes from an identification that the infrared limit, given by the energy scales $E \to 0$, is naively the same as the coupling $g^2 \to \infty$ limit. In practice, one always has an upper cutoff either from a truncation of the Hilbert space to diagonalize the

*nkarthik.work@gmail.com
†rajamani.narayanan@fiu.edu
‡sruthi81294@gmail.com

Hamiltonian associated with a timelike direction, or from the inverse lattice spacing, which can obscure the $g^2 \to \infty$ limit.

In this work, we impose the ultraviolet regulator using a lattice discretization and study the infrared limit carefully. We will work within the Euclidean lattice formalism, where the flavor symmetry remains intact. Furthermore, we will use exact chiral fermions on the lattice even away from the continuum limit, which will result in the full flavor symmetry of the left- and right-chiral currents. Of particular interest to us in this paper will be the scaling dimension of the scalar mesons,

$$M_{ij}(x) = \psi^{\dagger}_{iL}(x)\psi_{jR}(x) + \psi^{\dagger}_{iR}(x)\psi_{jL}(x); \tag{1}$$

where the color indices that are summed over are suppressed and only the flavor indices, $i, j = 1, \ldots, N_f$, are explicitly shown.

We plan to study $SU(N_c)$ gauge theories with exactly massless fermions using the lattice formalism in this paper. Since there are no topological zero modes, the one-point function will be exactly zero in any gauge field background, and we do not need to distinguish between $SU(N_f)$ scalars and the $U(1)$ scalar. In this case, the expected scaling dimensions of M_{ij} are that of a $u(N_f)$ WZW model with level N_c, and we cannot directly use the formula for the scaling dimension in [4]. To that end, we provide a derivation of the formula for the scaling dimensions of the scalar mesons within the context of the WZW model in Sec. II. This is followed by a description of the lattice formulation of two-dimensional QCD with exactly massless fermions in Sec. III. The dimensionless length of the symmetric Euclidean torus, l, will be the only parameter in the continuum limit of the lattice formalism. We will use the low-lying eigenvalues of the massless lattice Dirac operator and the meson correlator to show that the scaling dimension associated with the WZW algebra matches the behavior as $l \to \infty$ in Sec. IV. In addition, we will also study the vector meson (current) correlator and show that it remains invariant under the flow from ultraviolet to infrared.

II. WZW ALGEBRA

The Wess-Zumino-Witten model [5] of relevance to us is given by the action

$$S^{U(N_f)}_{N_c} = \frac{N_c}{16\pi}\int d^2x\, \mathrm{Tr}(\partial^{\mu} g^{-1}\partial_{\mu} g) + N_c\Gamma; \tag{2}$$

where $g \in U(N_f)$ is identified as the affine-primary[1] field in the CFT and Γ is the Wess-Zumino term given by

$$\Gamma = -\frac{i}{24\pi}\int_C d^3y\, \epsilon_{\alpha\beta\gamma}\mathrm{Tr}(\tilde{g}^{-1}\partial^{\alpha}\tilde{g}\tilde{g}^{-1}\partial^{\beta}\tilde{g}\tilde{g}^{-1}\partial^{\gamma}\tilde{g}). \tag{3}$$

This is understood as an integral over a three-dimensional manifold C where $\tilde{g}$ is the extension of the primary fields to this manifold. Note that the level of this WZW model is given by $\frac{N_c}{2}$. The infrared limit of the mesons, M_{ij}, is expected to be associated with g so our aim, in this section, is to obtain an expression for the scaling dimension of g. It is possible to extract this from a formula in [5] but we provide some details because the group is neither simple nor semisimple.

This WZW model admits conserved flavor currents $J(z) = J_L(z); \bar{J}(\bar{z}) = J_R(\bar{z})$ (the left-chiral and right-chiral currents in Sec. I) which can be expressed in terms of g as

$$J_L(z) = -\frac{N_c}{2}\partial_z g g^{-1}; \quad J_R(\bar{z}) = \frac{N_c}{2} g^{-1}\partial_{\bar{z}} g. \tag{4}$$

The modes of these currents satisfy the affine Kac-Moody algebra given by

$$[J_{k_1 f_1 fR;Lg}; J_{k_2 f_2 fR;Lg}] = i f_{f_1 f_2 f_3} J_{(k_1+k_2) f_3 fR;Lg} + \frac{N_c k_1}{2}\delta(k_1 + k_2). \tag{5}$$

In what follows, we drop the dependence on $z, \bar{z}$ and just notate the chirality of the current. Most generally, one constructs a stress tensor from a bilinear of these currents as per the Sugawara construction

$$T = \sum_a C_a :J^a_L J^a_L: \tag{6}$$

where $:\ :$ denotes normal ordering and C_a are a set of constants picked to normalize the stress tensor such that it has the usual operator product expansion. Mode expanding the Sugawara stress tensor, as per standard two-dimensional CFT, one obtains the following identification of the Virasoro generators:

$$L_n = \sum_a C_a \Big[\sum_{k<0} J_{k\,L} J_{(n-k);\,L} + \sum_{k\geq 0} J_{(n-k);\,L} J_{k\,L}\Big]^a = \sum_a C_a L^a_n; \tag{7}$$

where the sum has been divided in order to impose the normal ordering and L^a_n is a notation that will be useful in what follows.

We want to know the explicit expression for the Sugawara stress tensor when the J^a_L are $u(N_f)$ currents. In this case, the stress tensor can be decomposed into two parts, one that has all the $su(N_f)$ information and a

[1]The primary with respect to the affine current defined in the theory.

$u(1)$ piece.[2] This should be reminiscent of the fact that extending from $su(N_f)$ to $u(N_f)$ requires adding a generator (the identity) that has a different scaling factor than the other generators. Computing the commutators of these modes gives, most generally,

$$[L_n, L_m] = (n-m)(N_c+N_f)C^2 \sum_{b=1}^{N_f^2-1} L^b_{n+m} + N_c C^2 L^0_{n+m} + \frac{N_c}{2}(N_c+N_f)C^2(N_f^2-1) + \frac{N_c^2}{2}C_0^2 \times \frac{n(n^2-1)}{6}\delta_{n+m}. \quad (8)$$

Here C denotes the $su(N_f)$ normalization and C_0 is the $u(1)$ normalization constant. Asserting that this has to be the usual Virasoro algebra, allows us to solve for the normalization constants and write the $u(N_f)$ Sugawara stress tensor as

$$T_{u(N_f)} = \frac{1}{N_c+N_f} \sum_{a=1}^{N_f^2-1} :J^a_L J^a_L: + \frac{1}{N_c} :J^0_L J^0_L: . \quad (9)$$

Now that we have the stress tensor, we can find the dimension of the primary g. This relies on the fact that in addition to an affine primary, g is also a Virasoro primary. In any two-dimensional CFT, the operator product expansion (OPE) of the stress tensor with a primary field φ is given by [5]

$$T(z)\varphi(w,\bar{w}) \sim \frac{h}{(z-w)^2}\varphi(w,\bar{w}) + \frac{1}{z-w}\partial_w\varphi(w,\bar{w}). \quad (10)$$

The conformal weight h of the primary is given by the coefficient of the most singular term. Therefore, if we compute the most singular term of the OPE between $T_{u(N_f)}(z)$ and the WZW primary $g(w,\bar{w})$, we can read off its weight. In a WZW model the OPE between the current and the primary field g is given by [5]

$$J^a(z)g(w,\bar{w}) \sim -\frac{T^a g(w,\bar{w})}{z-w}. \quad (11)$$

Combining this with the definition of the $u(N_f)$ stress tensor and using identities of the sums of products of the generators T^a, one finds the weight of the primary to be[3]

$$h_g = \frac{N_f^2-1}{2N_f(N_c+N_f)} + \frac{1}{2N_c N_f} = \frac{N_c N_f + 1}{2N_c(N_c+N_f)}. \quad (12)$$

Additionally, one can read off the central charge as $c = \frac{N_f(N_c N_f+1)}{N_c+N_f}$ which was verified in [6] via alternative methods.

In the following analysis, we concern ourselves with the scaling dimension of the scalar mesons given in (1). This operator can be written in terms of the WZW primary as $M_{ij}(x) = g_{ij} + g^\dagger_{ij}$. One expects the conformal two-point function of two mesons to have the behavior $\frac{1}{|x-y|^{2\Delta}}$ where $\Delta = 2h_g$ is the conformal dimension. In terms of Δ, the mass anomalous dimension is given by

$$\gamma_m = 1 - \Delta = \frac{N_c^2-1}{N_c(N_c+N_f)}. \quad (13)$$

Our numerical results are for $(N_c, N_f) = (2,1), (2,2), (3,1), (3,2)$, and the specific values of Δ are $\frac{1}{2}, \frac{5}{8}, \frac{1}{3}, \frac{7}{15}$ respectively.

III. LATTICE FORMALISM

A. Lattice action and Monte Carlo simulation

We study the theory on a finite two-dimensional Euclidean periodic box of physical extent $l \times l$, where l is the dimensionless length measured in units of the 't Hooft coupling. Let the lattice be denoted as $L \times L$ where we assume L to be even. We will obtain the continuum limit at a fixed value of l by extrapolating the results obtained at a few finite values of L in the limit as $L \to \infty$. The lattice path integral for the two-dimensional QCD coupled to N_f flavors of massless fermions is

$$Z = \int \prod_{x,\mu} dU_\mu(x) \, (\det D_o)^{N_f} e^{S_g}, \quad (14)$$

where D_o is the overlap Dirac operator. S_g is the plaquette gauge action which is written in terms of gauge links $U_\mu(x)$ below:

$$S_g = \frac{N_c}{l^2}\sum_x \left(2N_c - P(x) - P(x)^\dagger\right)_x$$
$$P(x) = \mathrm{Tr}\left(U_1(x)U_2(x+\hat{1})U_1^\dagger(x+\hat{2})U_2^\dagger(x)\right), \quad (15)$$

where the trace is over color. To see the connection with the standard way to introduce lattice coupling in the action, note that $l = \sqrt{\lambda} l_{ph}$ where λ is the dimensionful 't Hooft coupling and l_{ph} is the dimensionful length. Then $\frac{N_c L^2}{l^2} = \frac{1}{(ga)^2}$ where $\lambda = g^2 N_c$ and $a = l_{ph}/L$ is the

[2] Usually one says that when you have a semisimple Lie algebra, the Sugawara stress tensor is the sum of the stress tensors for each simple Lie algebra. However, $U(N)$ is not semisimple, so we cannot make that argument here.

[3] We note that Jaume Gomis has independently verified this formula via a private communication.

lattice spacing. The overlap-Dirac [7–9] operator D_o can be written as

$$D_o = \frac{1 + V}{2}; \tag{16}$$

in terms of a unitary operator $V = \sigma_3 \epsilon(H_w)$ written in terms of the sign-function ϵ and the Hermitian Wilson-Dirac operator $H_w = \sigma_3 D_w$. We approximated the sign function using a 21-pole Zolotarev rational approximation. In two dimensions, the Wilson-Dirac operator that enters the construction of the overlap operator can be written as

$$D_w = (2 - M) - \frac{1}{2}[(1 - \sigma_1)T_1 + (1 + \sigma_1)T_1^\dagger + (1 - \sigma_2)T_2 + (1 + \sigma_2)T_2^\dagger]; \tag{17}$$

where the Wilson mass $M \in (0, 2)$. We set $M = 1$ in this study. In the above equation, σ_μ are the Pauli matrices, and T_1 and T_2 are the gauge covariant parallel transporters,

$$\begin{aligned} (T_\mu \varphi)(x) &= U_\mu(x)\varphi(x + \hat{\mu}); \\ (T_\mu^\dagger \varphi)(x) &= U_\mu^\dagger(x - \hat{\mu})\varphi(x - \hat{\mu}). \end{aligned} \tag{18}$$

In two dimensions, the lack of topological sectors in the $su(N_c)$ theory implies that there are no topological zero modes for the overlap Dirac operator. This lets us make the following simplification: noting that

$$H_o = \sigma_3 D_o = \frac{\sigma_3 + \epsilon(H_w)}{2}; \qquad [H_o^2, \sigma_3] = 0; \tag{19}$$

we can write

$$\det D_o = \det H_o = \det_+ H_o^2 = \det_- H_o^2; \tag{20}$$

where $+$ restricts the determinant to one chiral sector. We used the standard Hybrid Monte Carlo (HMC) algorithm [10] to sample gauge configuration weighted according to Eq. (14). Whereas the implementation of the HMC trajectories via the leap frog method is standard, we note the following interesting feature. The fermionic action using N_f copies of pseudofermions φ_{i+} is given by

$$S_f(\varphi) = \sum_{i=1}^{N_f} \varphi_{i+}^\dagger \frac{1}{H_o^2} \varphi_{i+}; \qquad \sigma_3 \varphi_{i+} = \varphi_{i+}. \tag{21}$$

In the above equation, by restricting the action to a single chiral sector, we are able to write the action in terms of a positive definite operator for each flavor, which thereby enables us to set N_f to any value. The details about the algorithm are the same as the one employed in the study of three-dimensional QED in [11].

B. Lattice observables to probe the conformal infrared behavior

We study the scaling dimension of the scalar operator using the two-point function, as well as by probing the finite-size scaling of the low-lying eigenvalues of the overlap Dirac operator. In addition, we will also study the correlator of the vector meson in order to show that it does not acquire an anomalous dimension. Both the scalar and vector meson correlators can be written in terms of the anti-Hermitian massless overlap fermion propagator,

$$G_o = \frac{1 - V}{1 + V}. \tag{22}$$

We first notice that $\{G_o, \sigma_3\} = 0$, implying that the form of the overlap propagator is

$$G_o = \begin{pmatrix} 0 & G_L \\ -G_L^\dagger & 0 \end{pmatrix}; \tag{23}$$

where G_L is the propagator of the left-chiral fermion and $-G_L^\dagger$ is the propagator of the right-chiral fermion.

Observables with better sensitivity to the infrared conformality are the microscopic low-lying eigenvalues of the Dirac operator. For the overlap operator, they are the eigenvalues of the inverse of the overlap propagator $A = G_o^{-1}$, given by

$$A v_j = i\Lambda_j v_j; \tag{24}$$

determined over a fixed gauge field background. Since eigenvalues come in positive-negative pairs, we can take $\Lambda_j > 0$ in the above equation, and the eigenvalues are sorted as $\Lambda_{j+1} > \Lambda_j$ for $j = 1; \ldots; N_c L^2$. We will only consider the first few values of $j = 1, 2, 3, 4$ in this study.

We measured Λ_j in the sampled gauge configurations, and determined the ensemble averages $\langle \Lambda_i \rangle$. The continuum limits $\lambda_i(l)$ of the eigenvalues are given by

$$\lambda_i(l) \equiv \lim_{L \to \infty} \langle \Lambda_i \rangle L. \tag{25}$$

The dependence of the scalar susceptibility (i.e., scalar correlator integrated over the entire box), gives the corresponding expectation for the finite-size scaling of $\lambda_i(l)$. Namely, again anticipating a free-theory-like short-distance behavior and a nontrivial conformal behavior in the infrared given by (13), we expect

$$\begin{aligned} &\lambda_i(l) \propto l^0 \quad \text{as } l \to 0; \quad \text{and} \quad \lambda_i(l) \propto \frac{1}{l^{\gamma_m}}; \\ &\gamma_m = \frac{N_c^2 - 1}{N_c(N_f + N_c)} \quad \text{as } l \to \infty. \end{aligned} \tag{26}$$

Next, we turn our attention to meson correlators. At a fixed value of l, the lattice scalar and vector meson correlators will be periodic functions that depend on the lattice separation, x. Upon taking the continuum limit, the correlators will naturally become a function of $\xi = x = l = \lim_{L\to\infty} x/l$. Usually, one studies the correlator as a function of x as $l \to \infty$, which amounts to the behavior as $\xi \to 0$ at fixed $\xi l = x$. In this limit, one recovers the correlators of operators O on an infinite plane, which will behave as $C_O = x^{2\Delta_O}$ in the UV and IR limits, with the appropriate UV and IR values of the scaling dimensions Δ_O. The coefficients of the power-law dependence, C_O^{UV} and C_O^{IR}, in the two limits, are referred to as the UV and IR amplitudes. We can instead study the behavior of the correlators as a function of l at a fixed $\xi > 0$ (see for example [11]). On a periodic torus, the correlators will still behave as power law in operator separation ξl in the large and small l limits, and the power-law coefficients generalize into functions of ξ and l that approach their UV and IR limits, $C_O^{UV}(\xi)$ and $C_O^{IR}(\xi)$. The amplitudes of the power law on an infinite plane are then recovered from $C_O^{UV;IR}(\xi)$ in the $\xi \to 0$ limit. In this work, we focus on these coefficients at a finite ξ and study their flow from UV to IR to avoid additional, difficult $\xi \to 0$ extrapolation. Below, we apply this general discussion to the specific cases of the scalar meson and vector meson (conserved current) correlators.

In terms of G_L, we write the continuum pseudoscalar and the left-chiral and the right-chiral current correlators as

$$l^2 G_s(l;\xi) = \frac{1}{G_f(\xi)} \lim_{L\to\infty} L^2 \langle \mathrm{Tr}[G_L(0;L\xi) G_L^\dagger(0;L\xi)] \, G_L(L\xi;0) G_L^\dagger(L\xi;0)\rangle;$$

$$l^2 G_v(l;\xi) = \frac{1}{G_f(\xi)} \lim_{L\to\infty} L^2 \langle \mathrm{Tr}[G_L(0;L\xi) G_L(0;L\xi)] \, G_L^\dagger(L\xi;0) G_L^\dagger(L\xi;0)\rangle : \quad (27)$$

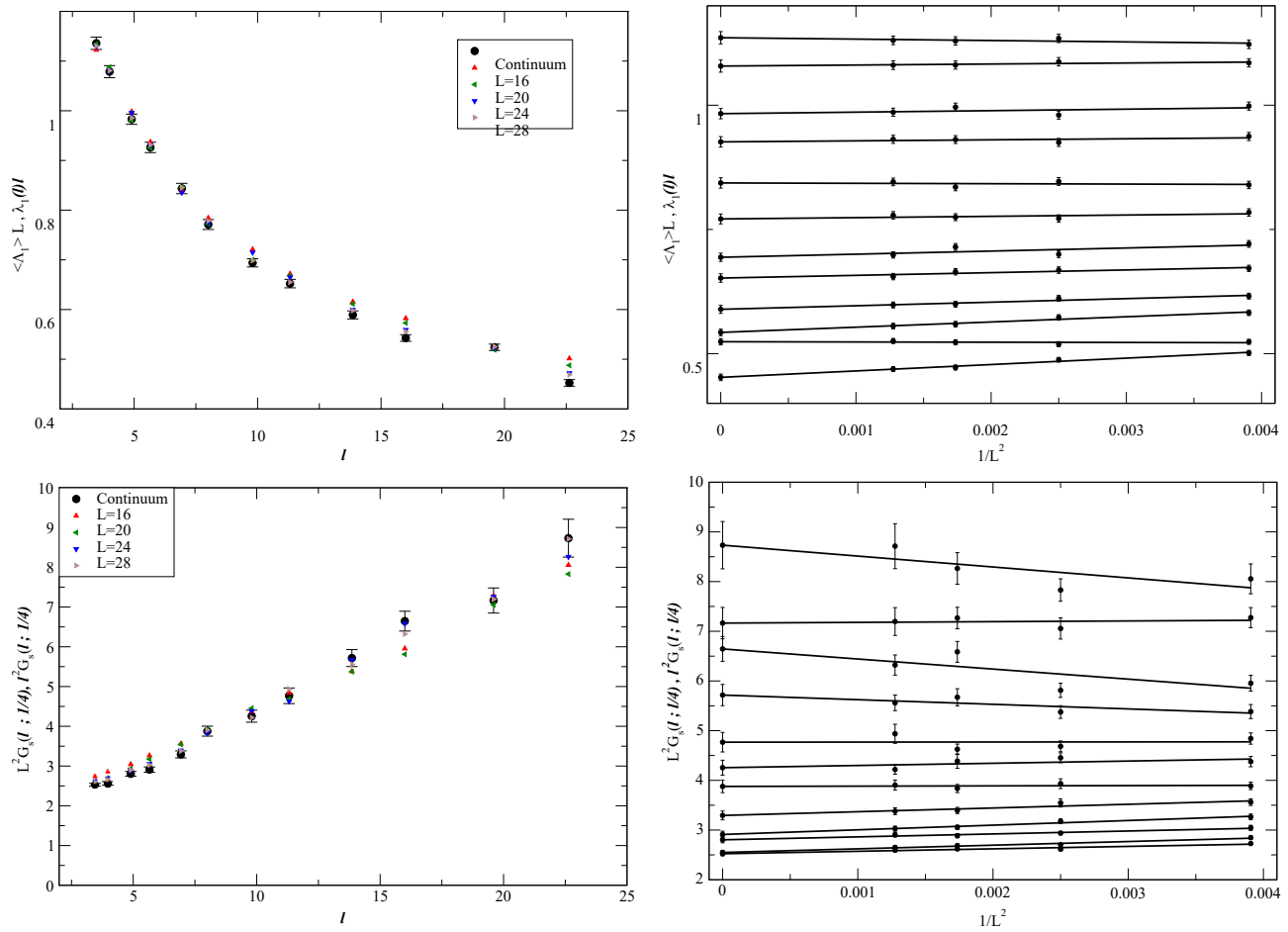

FIG. 1. The lowest eigenvalue (top panels) and the scalar correlator (bottom panels) after appropriate l scaling are shown as a function of l (left panels) and function of L (right panels) for a representative case $(N_c; N_f) = (2; 1)$. Only the central values of the data are shown at four values of the lattice extent L in the left panels to avoid clutter, and they are compared against the continuum extrapolated values shown as black-filled circles. The right panels include the errors at each L and show the fit to extract the continuum values.

The trace is only over the color indices. The factor l^2 multiplying the correlator on the left accounts for the naïve scaling dimension from units of lattice spacing to the units of the coupling. The free correlator, $G_f(\xi)$ is specific to the overlap-Dirac operator and is defined as

$$G_f(\xi) = \lim_{L\to\infty} L^2 \langle G_{fL}(0;L\xi) G^\dagger_{fL}(0;L\xi) \rangle + G_{fL}(L\xi;0) G^\dagger_{fL}(L\xi;0); \quad (28)$$

where G_{fL} is the free fermion propagator. The free correlator will be proportional to $\frac{1}{\xi^2}$ when $\xi \to 0$. Note that we have divided the correlators by $G_f(\xi)$ in Eq. (27) to take care of continuum-like normalization, and to avoid trivial factors of $\frac{1}{\xi^2}$.

We can define amplitudes at finite l and ξ from correlators by scaling with appropriate powers of $x = \xi l$. The scalar correlator is anomalous, and we will need to use two different scalings in the ultraviolet and infrared to define appropriate amplitudes, namely,

$$C^{UV}_s(l;\xi) = l^2 G_s(l;\xi)$$
$$C^{IR}_s(l;\xi) = (\xi l)^{-2\gamma_m} l^2 G_s(l;\xi): \quad (29)$$

Then, $C^{UV}_s(0;\xi)$ and $C^{IR}_s(\infty;\xi)$ will give us the amplitudes in the ultraviolet and infrared. In contrast, the vector meson correlator has the same scaling dimension in the ultraviolet and infrared, and we define its amplitude as

$$C_v(l;\xi) = l^2 G_v(l;\xi): \quad (30)$$

Then, $C_v(0;\xi)$ and $C_v(\infty;\xi)$ will give us the amplitudes in the ultraviolet and infrared. In this work, we will study the behavior of the RG flow of $C^{UV}_s(l;\xi)$, $C^{IR}_s(l;\xi)$ and $C_v(l;\xi)$ at a fixed value of $\xi = 1/4$.

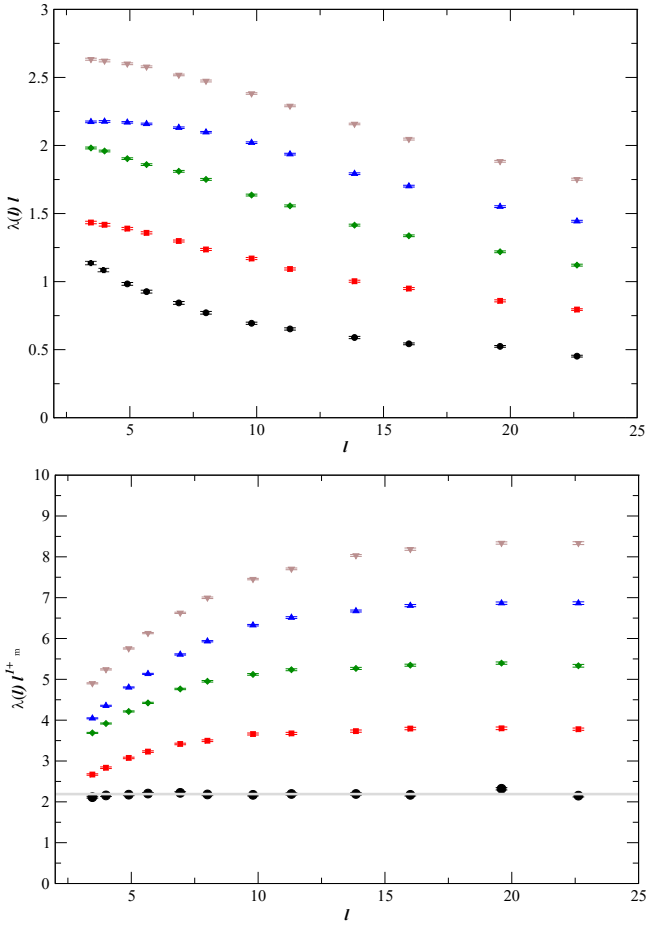

FIG. 2. The five lowest eigenvalues are plotted as a function of l for $N_c = 2$ and $N_f = 1$. The top panel is scaled as per the naive ultraviolet scaling, and the bottom panel is scaled as per the predicted infrared scaling using the appropriate WZW model, namely, $\gamma_m = \frac{1}{2}$.

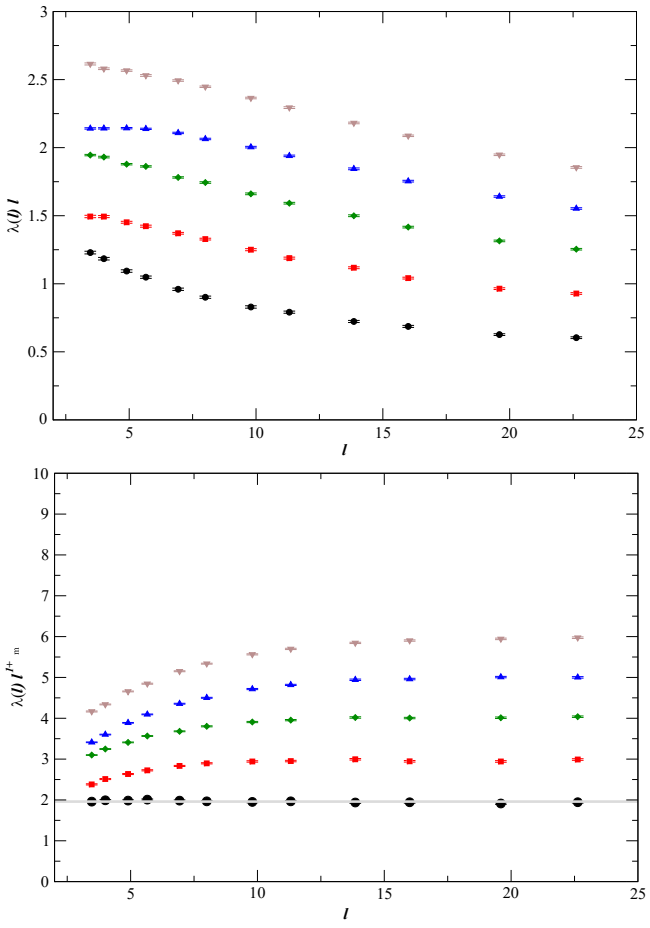

FIG. 3. The five lowest eigenvalues are plotted as a function of l for $N_c = 2$ and $N_f = 2$. The top panel is scaled as per the naive ultraviolet scaling, and the bottom panel is scaled as per the predicted infrared scaling using the appropriate WZW model, namely, $\gamma_m = \frac{3}{8}$.

IV. RESULTS

The numerical analysis parallels methods used in the study of three-dimensional massless QED in [11], and we do not provide the details here. We used lattices with $L = 16, 20, 24, 28$ in our numerical simulations. We studied the theories with $(N_c, N_f) = (2, 1), (2, 2), (3, 1), (3, 2)$. At each L, we performed Monte Carlo simulations at the following values of dimensionless areas l^2:

$$l^2 = 12, 16, 24, 32, 48, 64, 192, 256, 384, 512 \quad \text{for } N_c = 2;$$
$$l^2 = 15, 24, 30, 48, 63, 96, 126, 192, 384 \quad \text{for } N_c = 3: \tag{31}$$

The values chosen were arbitrary, but cover small-box sizes that are likely to be closer to ultraviolet behavior, and larger box sizes that are likely to be in the basin of the infrared behavior. At each simulation point, we generated around 5000 trajectories, and we measured the eigenvalues and the fermion correlators every five trajectories to account for autocorrelations. Furthermore, we divided the measurements into 200 jack-knife blocks to estimate the mean and statistical errors of the observables. We determined the continuum limits of the eigenvalues and the two correlators at each fixed l by fitting the data from the four values of L using a functional form $A + \frac{B}{L^2}$ with fit parameters A and B, and extrapolating to $L \to \infty$ limit (i.e., the fitted value of A). The first lattice correction arises at $O(1/L^2)$ due to the exact chiral symmetry of the lattice overlap fermion. The finite L effects are small for the observables studied in this paper, and Fig. 1 shows the lowest eigenvalue and the scalar correlator at $(N_c, N_f) = (2, 1)$ as a sample.

We show the finite-size dependence of the lowest five eigenvalues in Figs. 2–5 for $(N_c, N_f) = (2, 1), (2, 2), (3, 1), (3, 2)$ cases respectively. As l goes from the smallest value to the largest value, we expect a flow from the naive ultraviolet behavior to the infrared behavior predicted by the WZW model in Sec. II. To verify that this is indeed the

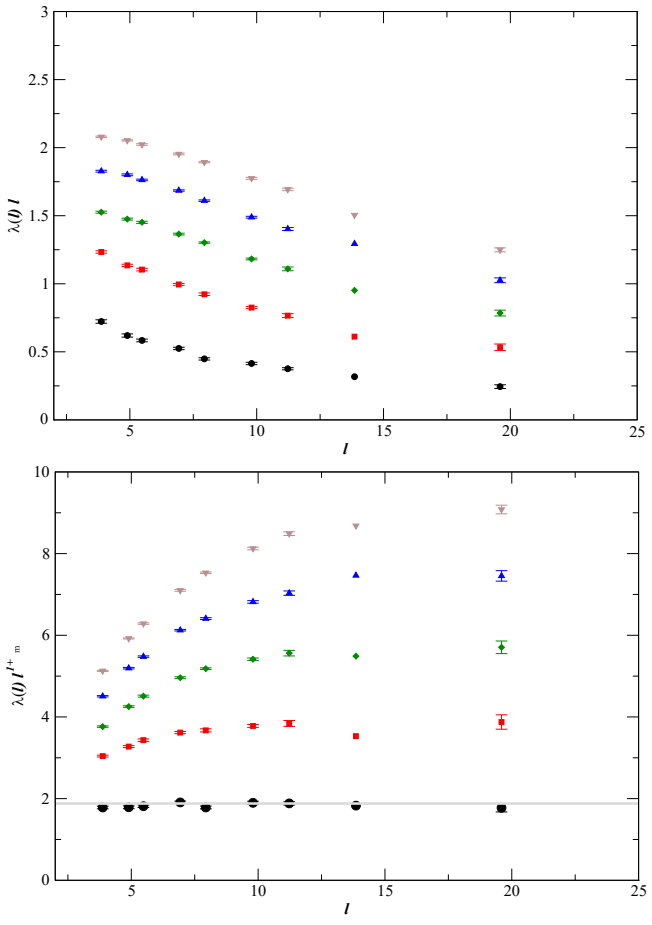

FIG. 4. The five lowest eigenvalues are plotted as a function of l for $N_c = 3$ and $N_f = 1$. The top panel is scaled as per the naive ultraviolet scaling, and the bottom panel is scaled as per the predicted infrared scaling using the appropriate WZW model, namely, $\gamma_m = \frac{2}{3}$.

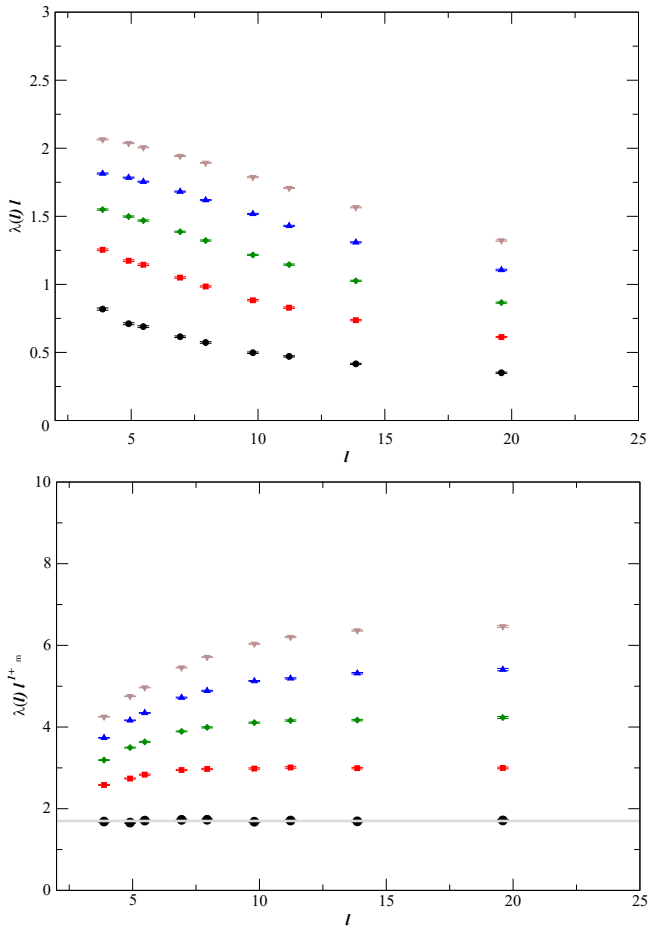

FIG. 5. The five lowest eigenvalues are plotted as a function of l for $N_c = 3$ and $N_f = 2$. The top panel is scaled as per the naive ultraviolet scaling, and the bottom panel is scaled as per the predicted infrared scaling using the appropriate WZW model, namely, $\gamma_m = \frac{8}{15}$.

case, we have plotted $\lambda_i(l)l$ in the top panels and $\lambda_i(l)l^{1-\gamma_m}$ in the bottom panels. If the expected ultraviolet and infrared behavior sets in, we should see these appropriately scaled eigenvalues approach a plateau as a function of l (for small l in the top panels, and larger l in the bottom panels). In all four cases studied in this paper, we observe that even the smallest l used in the study shows the expected infrared behavior of the lowest eigenvalue, $\lambda_1(l)l$. To emphasize that $\lambda_1(l)l^{1-\gamma_m}$ remains a constant throughout the range of l considered in this paper, we have drawn a horizontal line through the points to guide the eye. This is clear evidence that γ_m for the infrared CFT matches that of a WZW model. The second and fourth eigenvalues seem to approach the naive ultraviolet behavior for the smallest l studied here. On the other hand, the bottom panels clearly show that $\lambda_i(l)l$ for $i = 2, 3, 4, 5$ flow toward the expected infrared behavior as one approaches large values of l and the lower eigenvalues approach the infrared behavior faster than the higher eigenvalues. That the case of $(N_c, N_f) = (3, 1)$ has an underlying supersymmetry [4] does not seem to single out the flow.

We discuss the flow of the two-point functions below, starting from the conserved vector mesons. In Fig. 6, we show the continuum extrapolated amplitude, $C_v(l, \xi)$ at $\xi = \frac{1}{4}$ computed in the interacting theory. This quantity should flow from its ultraviolet value at small l to its infrared value at large l, with perhaps a crossover between the ultraviolet and infrared behavior at some intermediate l. However, we note a clear plateau over the entire range of l we studied with no sign of such a UV-IR crossover. This is consistent with the expectation that the vector meson amplitude is a renormalization group invariant, namely,

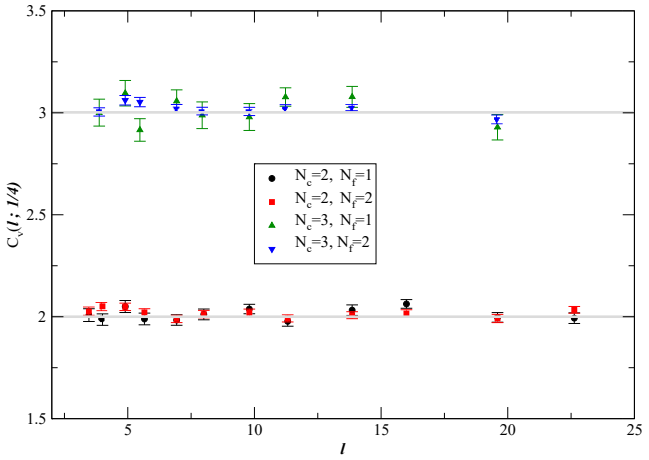

FIG. 6. The flow of the amplitude of the vector meson correlator, as defined in Eq. (30). The figure shows the l dependence of $C_v(\xi; l)$ that should plateau at the UV amplitude for small l, and should also plateau at the IR amplitude for large l. The data from four different $(N_f; N_c)$ are shown using a specific $\xi = 1/4$. The horizontal lines are shown to indicate the absence of a UV-IR flow of the vector meson amplitude.

$C_v(l; \xi = 0)$ is independent of l, owing to the 't Hooft anomaly matching condition for the global flavor symmetry [4]. This behavior could be contrasted with the renormalization group flow of the current amplitudes in three-dimensional massless QED (see for instance [12,13].) We also notice that there is no dependence of the data points in Fig. 6 on N_f, and the value of $C_v(\infty; \frac{1}{4})$ is consistent with N_c, as expected of the WZW model.

Note that the distinction between $U(N_f)$ and $SU(N_f)$ is not relevant at the level of current correlators in a WZW model. One should note that the free correlator, $G_f(\xi)$ is independent of N_c and N_f, and hence, the ratio of 3=2 between the amplitudes is not imposed by hand.

In the following discussion, we return to the scaling dimension of the scalar operator, now discussed using the scalar correlator. In Fig. 7, we show the l dependence of the $C_s^{UV;IR}(l; \xi)$ at a fixed value of $\xi = \frac{1}{4}$. The ultraviolet

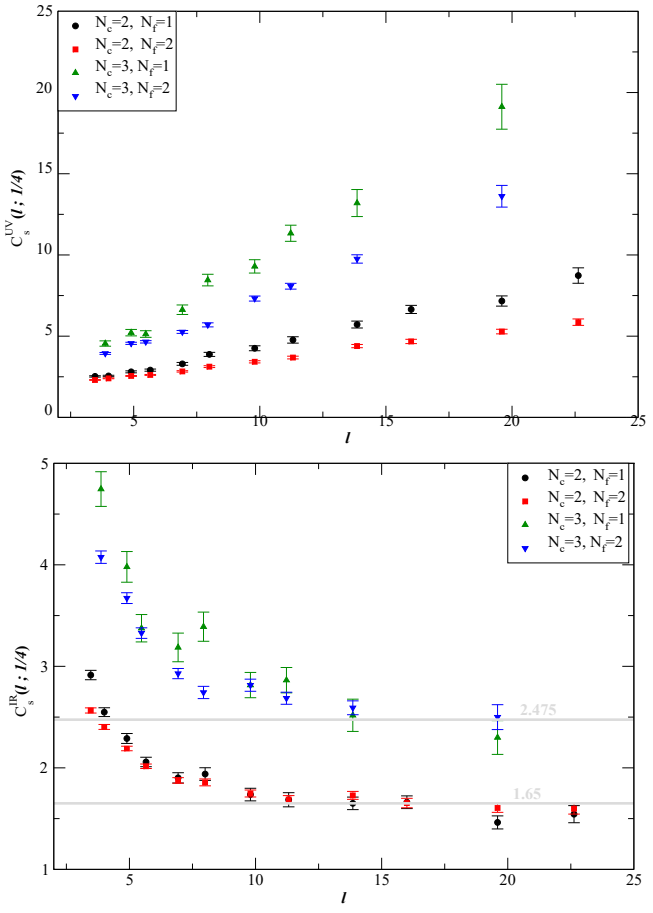

FIG. 7. The flow of the amplitude of the scalar correlator, as defined in Eq. (29) by a UV scaling (top panel) and by WZW infrared scaling (bottom panel) of the scalar correlator. The top panel shows the l dependence of $C_s^{UV}(\xi; l)$ that should plateau at the UV amplitude for small l. The bottom panel shows the l dependence of $C_s^{IR}(\xi; l)$ that should plateau at the IR amplitude for large l. The data from four different $(N_f; N_c)$ are shown using a specific $\xi = 1/4$.

behavior is highlighted in the top panel, and the infrared behavior is highlighted in the bottom panel. We should see a plateau in the top panel for small l if we are close to the basin of the ultraviolet, free CFT. Like in the case of the eigenvalues, the smallest value of l studied here is still away from the naive ultraviolet limit, as is evident from the residual l dependence at small l seen in the top panel. Unlike the vector meson correlator, we see a distinct UV-IR flow in the data points in the bottom panel. The apparent plateau for large values of l is again evidence for the approach to a WZW model in the infrared. Like in the case of the vector meson amplitudes, we see that the scalar amplitudes in the infrared are independent of N_f and scale linearly with N_c.

V. CONCLUSIONS

We have studied two-dimensional $\mathrm{su}(N_c)$ gauge theories with N_f flavors of massless fermions using the lattice formalism with exact massless fermions on the lattice. We aimed to supplement the analysis usually performed in the Discrete Light-Cone Hamiltonian. In particular, we studied the mass anomalous dimensions and the related scaling dimensions of scalar mesons, which require the presence of both left-chiral and right-chiral conserved flavor currents. Flavor symmetry is exact in our lattice formalism, and our numerical studies with $(N_c, N_f) = (2,1), (2,2), (3,1), (3,2)$ clearly show the expected scaling in the infrared given by the appropriate WZW model. We also see a flow from the ultraviolet to the infrared. We find evidence of the amplitude of the conserved current correlator being renormalization group invariant, as expected from the anomaly matching condition. In contrast, we see a distinct UV-IR flow of the amplitude of the scalar correlator with these amplitudes approaching N_f-independent values in the infrared. Our work closes a conjectural gap in the recent studies on the classification of infrared phases of QCD by removing the ultraviolet lattice regulator first before taking the infrared limit.

ACKNOWLEDGMENTS

The authors thank Jaume Gomis for useful discussions. R. N. acknowledges partial support by the NSF under Grants No. PHY-1913010 and No. PHY-2310479. S. N. acknowledges support by the Celestial Holography Initiative at the Perimeter Institute for Theoretical Physics and by the Simons Collaboration on Celestial Holography. S. N′s research at the Perimeter Institute is supported by the Government of Canada through the Department of Innovation, Science and Industry Canada and by the Province of Ontario through the Ministry of Colleges and Universities. This work used Expanse at SDSC through allocation PHY220077 from the Advanced Cyberinfrastructure Coordination Ecosystem: Services & Support (ACCESS) program, which is supported by National Science Foundation Grants No. 2138259, No. 2138286, No. 2138307, No. 2137603, and No. 2138296.

[1] D. Delmastro, J. Gomis, and M. Yu, J. High Energy Phys. 02 (2023) 157.
[2] K. Hornbostel, S. J. Brodsky, and H. C. Pauli, Phys. Rev. D 41, 3814 (1990).
[3] K. Hornbostel, Ph.D. thesis, Stanford University, 1988.
[4] D. Delmastro and J. Gomis, J. High Energy Phys. 09 (2023) 158.
[5] P. Di Francesco, P. Mathieu, and D. Senechal, Conformal Field Theory, Graduate Texts in Contemporary Physics (Springer-Verlag, New York, 1997), ISBN 978-0-387-94785-3, 978-1-4612-7475-9.
[6] S. G. Naculich and H. J. Schnitzer, J. High Energy Phys. 06 (2007) 023.
[7] R. Narayanan and H. Neuberger, Nucl. Phys. B443, 305 (1995).
[8] H. Neuberger, Phys. Lett. B 417, 141 (1998).
[9] R. G. Edwards, U. M. Heller, and R. Narayanan, Phys. Rev. D 59, 094510 (1999).
[10] S. Duane, A. Kennedy, B. Pendleton, and D. Roweth, Phys. Lett. B 195, 216 (1987).
[11] N. Karthik and R. Narayanan, Phys. Rev. D 94, 065026 (2016).
[12] S. Giombi, G. Tarnopolsky, and I. R. Klebanov, J. High Energy Phys. 08 (2016) 156.
[13] N. Karthik and R. Narayanan, Phys. Rev. D 96, 054509 (2017).